N O T I C E

THIS DOCUMENT HAS BEEN REPRODUCED FROM MICROFICHE. ALTHOUGH IT IS RECOGNIZED THAT CERTAIN PORTIONS ARE ILLEGIBLE, IT IS BEING RELEASED IN THE INTEREST OF MAKING AVAILABLE AS MUCH INFORMATION AS POSSIBLE

NASA Technical Memorandum 81303

USAAVRADCOM TR 81-B-18

(NASA-TM-81303) PREDICTION OF BOUNDARY-LAYER CHARACTERISTICS OF AN OSCILLATING AIRFOIL (NASA) 17 p HC A02/MF A01 CSCL 20D

N81-28391

Unclas

G3/34 27021

# Prediction of Boundary-Layer Characteristics of an Oscillating Airfoil

Tuncer Cebeci and Lawrence W. Carr

July 1981

RECEIVED
NASA STI FACILITY
ACCESS DEPT.

National Aeronautics and
Space Administration

United States Army
Aviation Research
and Development
Command

NASA Technical Memrandum 81303 USAAVRADCOM TR 81-3-18

# Prediction of Boundary-Layer Characteristics of an Oscillating Airfoil

Tuncer Cebeci, Mechanical Engineering Department
California State University, Long Beach, California

Lawrence W. Carr, Aeromechanics Laboratory
AVRADCOM Research and Technology Laboratories
Ames Research Center, Moffett Field, California

NASA
National Aeronautics and
Space Administration

**Ames Research Center**
Moffett Field, California 94035

United States Army
Aviation Research
and Development
Command

# PREDICTION OF BOUNDARY-LAYER CHARACTERISTICS OF AN OSCILLATING AIRFOIL *

Tuncer Cebeci and Lawrence W. Carr

Mechanical Engineering Dept.
California State University
Long Beach, California

U.S. Army Aeromechanics Lab.
NASA Ames Research Center
Moffett Field, California

## Abstract

The evolution of unsteady boundary layers on oscillating airfoils is investigated by solving the governing equations by the Characteristic Box scheme. The difficulties associated with computing the first profile on a given time-line, and the velocity profiles with partial flow reversal are solved. A sample calculation has been performed for an external velocity distribution typical of those found near the leading edge of thin airfoils. The results demonstrate the viability of the calculation procedure.

## Introduction

The effect of unsteady motion of an airfoil on its stall behavior is a problem of great importance in many types of fluid motion, for example, helicopter rotor blades and jet engine compressors. A recent detailed study has been published by Carr, McAlister and McCroskey(1); this study reveals a very complicated phenomenon which depends in a subtle way on a large number of parameters. There is one important characteristic of the data they have compiled which serves as a focal point of the approach which we are planning to apply sometime later in our studies; namely that at some stage of the cycle, a large vortex is formed near the surface of the airfoil and very shortly afterwards stall occurs. It seems also that the stall is associated with flow reversals in the unsteady boundary layer which may spread downstream or upstream depending on the leading-edge radius of the airfoil.

The present paper concerns itself with the calculation of boundary-layer characteristics of an oscillating airfoil in order to investigate the evolution of unsteady boundary layers on such airfoils. It is one phase of a study which will be extended later in the hope of throwing light on the dynamic stall problem. In our present study we focus our attention on

*Presented at the IUTAM Symposium on Unsteady Turbulent Shear Flows, Toulouse, 5-8 May 1981.

the calculation of time-dependent boundary layers for a given pressure distribution.

There are three difficulties associated with unsteady boundary layers that requires careful attention. First of all appropriate initial values at $t = 0$ must be chosen for the velocity distribution. Strictly speaking they can be arbitrary but in that event, the values of $\partial u/\partial t$ at $t = 0$ is non-zero and this implies an inviscid acceleration of the fluid in the boundary layer and in consequence a velocity of slip begins to grow at the wall. This is smoothed out by an inner boundary layer initially of thickness $(\nu t)^{1/2}$ in which viscous forces are of importance. Thus a double structure develops in the boundary layer which may be treated by a generalization of the Keller-box scheme[2]. However, if interest is centered on the solution at large times, this feature may be reduced in importance by requiring that the initial velocity distribution satisfies the steady-state equation with the instantaneous external velocity. In addition it is necessary to smooth out the external velocity $u_e(x,t)$ so that $\partial u_e/\partial t = 0$ at $t = 0$ and then standard methods may be used and are stable. The use of the smoothing function makes for some loss of accuracy at small values of $t$ but the error soon decays to zero once the required value of $u_e$ is specified. In the present problem the choice of parameters in the specified external velocity distribution is such that the smoothing function is actually unnecessary but it can easily be incorporated into the scheme.

The second difficulty arises when $u$ changes sign over part of the profile at some x-station where the x-axis is parallel to the streamwise direction and $u$ is the corresponding velocity component. Normally this does not occur and one can integrate away from the profile in the direction of positive $u$ without any difficulty by using a standard numerical scheme. However, if the change in sign of $u$ does occur, we encounter numerical instabilities since in the negative u-region we would be integrating against the stream. The instability can be avoided by changing the scheme either to the zig-zag box or the characteristics box. These new schemes have already been shown to be effective in such circumstances when the flow is unsteady[3] and in three-dimensional flows[4-6]. The essence of these schemes is that, to an increasing extent, they take into account the fact that small disturbances are carried along with the <u>local</u> fluid velocity.

The third difficulty arises when it is desired to compute the first velocity profile at the new time line. Given, as we are, the complete velocity profile distribution on the previous time line, there is in principle no difficulty in computing values on the next time-line by an explicit method, but if we wish to avoid the stability problems associated with such a method by using an implicit method, we are immediately faced with the problem of generating a starting profile on the new time-line.

In order to explain the problem further, it is instructive to see what happens to the stagnation point as a function of time. For this purpose let us assume that the external velocity distribution for an oscillating airfoil is given by the following function,

$$u_e = \frac{x + \xi_0 (1 + A \sin \omega t)}{(1 + x^2)^{\frac{1}{2}}} \tag{1}$$

where $A$ and $\xi_0$ denote parameters that need to be specified. This equation is a good approximation to the external velocity distribution near the leading edge of a class of thin airfoils at variable angles of attack and, when $A = 0$, has recently been used by Cebeci, Stewartson, and Williams[7] to study leading-edge separation in steady flow.

Since by definition $u_e = 0$ at the stagnation point, its location, $x_s$, is given by

$$x_s = -\xi_0 (1 + A \sin \omega t) \tag{2}$$

and so the upper and lower surfaces of the airfoil as functions of time are defined in particular by $x > x_s$ and $x < x_s$. For example, let us take $A = 1$, $\omega = \pi/4$ and plot $x_s/\xi_0$ in the $(t,x)$ plane, as shown in Figure 1 for one cycle $(0 \leq t \leq 8)$. When $t = 2$, the stagnation point $x_s$ is at $-2\,\xi_0$, when $t = 6$ it is at 0, etc. If $x_s$ were fixed we could assume that $u = 0$ at $x = x_s$ for all time and all $y$. Further profiles at this time-line then follow by use of one of the box schemes that have been developed. However $x_s$ is not fixed and it is clearly unjustified to assume a priori that $u = 0$ there. Instead therefore we use the characteristic box, with an

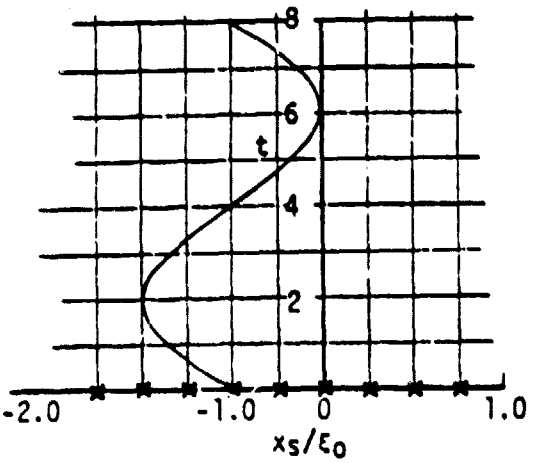


Fig. 1. Variation of stagnation point with time for one cycle according to Eq. (2), with $\omega = \pi/4$.

extrapolated normal velocity, to complete the profile at $x = x_1$, the nearest $x$ station to $x_s$ on the new time-line. Thus we avoid the need to use two x-stations at the new time-line to dimensionalize the governing equations. Once this step is completed, the determination of further profiles on the new time line proceeds normally and moreover we can improve our initial estimate of the normal velocity at $x = x_1$ by iteration.

## Governing Equations

The governing boundary-layer equations for an incompressible laminar or turbulent flow past an oscillating airfoil are well known and, with the eddy viscosity $(\varepsilon_m)$ concept, they can be written as

$$\frac{\partial u}{\partial x} + \frac{\partial v}{\partial y} = 0 \tag{3}$$

$$\frac{\partial u}{\partial t} + u\frac{\partial u}{\partial x} + v\frac{\partial u}{\partial y} = \frac{\partial u_e}{\partial t} + u_e\frac{\partial u_e}{\partial x} + \frac{\partial \tau}{\partial y} \tag{4}$$

where $\tau = \nu(\partial u/\partial y) - \overline{u'v'}$. In the absence of mass transfer, these equations are subject to the boundary conditions given by

$$y = 0, \quad u = v = 0; \quad y \to \delta, \quad u \to u_e(x,t) \tag{5}$$

The presence of the Reynolds shear stress term, $-\overline{u'v'}$, requires a closure assumption; in our study we use the algebraic eddy-viscosity formulation developed by Cebeci and Smith. For details, see ref. 8.

To complete the formulation of the problem, initial conditions must be specified in the $(t,y)$ plane at some $x = x_0$ either on the lower or upper surface of the airfoil (see Fig. 1) as well as initial conditions in the $(x,y)$ plane on both surfaces of the airfoil. In the latter case, if we assume that steady-flow conditions prevail at $t = 0$, then the initial conditions in the $(x,y)$-plane can easily be generated for both surfaces by

solving the governing equations for steady flow, which in this case, are given by Eq. (3) and by

$$u \frac{\partial u}{\partial x} + v \frac{\partial u}{\partial y} = u_e \frac{du_e}{dx} + \frac{\partial}{\partial y} \left(b \frac{\partial u}{\partial y}\right) \tag{6}$$

where $b = \nu + \varepsilon_m$. There is no problem with the initial conditions for Eqs. (1) and (6) since the calculations start at the stagnation point, $x = x_s$.

Generation of the initial conditions in the $(t,y)$ plane at $x = x_0$, which is one of the purposes of our study, is not so easy as was discussed in the previous section. The following section describes our solution procedure at $t = 0$ and $t > 0$.

## Solution Procedure

We use Keller's Box method to solve the governing equations of the previous section. This is a two-point finite-difference method which has been used to solve a wide range of parabolic partial-differential equations as discussed by Bradshaw, Cebeci and Whitelaw[9]. The solution procedure for $t = 0$ (Eqs. (3) and (6)) and $t > 0$ (Eqs. (3) and (4)) are described separately below.

## Solution Procedure for $t = 0$

As explained in the introduction any velocity profile may be chosen at $t = 0$ to initiate the computation but it is convenient to select one which obviates the need for double-structured numerical schemes and joins smoothly on to the solution for $t > 0$. We insist that these profiles satisfy the steady state equations with $u_e$ given by (1) and $t = 0$. The details of the procedure for computing these profiles differs slightly from previous procedures used in steady two-dimensional flows where we have used the definition of the stream function and reduced Eqs. (3) and (6) to <u>two</u> first-order ordinary differential equations and to <u>one</u> partial-differential equation. Here we consider the solution of Eqs. (3) and (6) without the use of the stream function. For this purpose, with primes denoting differentiation with respect to $y$, we let

$$u' = f \tag{7a}$$

and write Eqs. (3) and (6) as

$$v' = -\frac{\partial u}{\partial x} \tag{7b}$$

$$(bf)' - fv = -\frac{d}{dx}\left(\frac{u_e^2}{2}\right) + \frac{\partial}{\partial x}\left(\frac{u^2}{2}\right) \tag{7c}$$

The finite-difference approximations of Eqs. (7) are also somewhat different than those reported in our previous studies dealing with two-dimensional flows[10]. All quantities except for the normal velocity component $v$, are centered at the center of the box $(y_{j-1/2}, x_{i-1/2})$, see Fig. 2, by taking the values of each parameter, say $q$, at the four corners of the Box, that is,

$$q_{j-1/2}^{i-1/2} = \frac{1}{2}\left(q_j^{i-1/2} + q_{j-1}^{i-1/2}\right) = \frac{1}{4}\left(q_j^i + q_j^{i-1} + q_{j-1}^i + q_{j-1}^{i-1}\right) \tag{8a}$$

However, the centering of the y-velocity component $v$ is done by writing it as

$$v_{j-1/2}^{i-1/2} = \frac{1}{2}\left(v_j^{i-1/2} + v_{j-1}^{i-1/2}\right) \tag{8b}$$

The unknown parameters in Eqs. (8) correspond to $q_j^i$ and $v_j^{i-1/2}$ so that when a solution of the system given by Eqs. (7) is obtained, $f$ and $u$ are computed at $(i,j)$ and $v$ at $(i-1/2, j)$. This modified centering procedure is necessary in order to avoid oscillations due to the use of the continuity equation in the form given by Eq. (7b) rather than the use of the stream function. The centering of Eqs. (7) and the subsequent linearization procedure by Newton's method allows the resulting linear system to be written in the form[10]

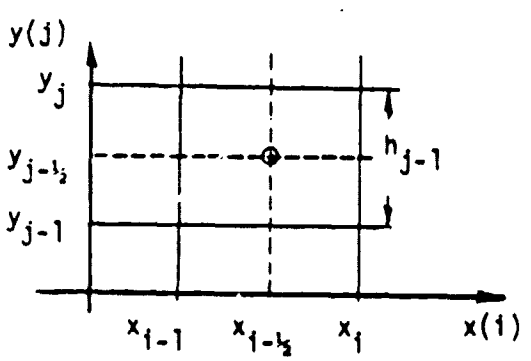


Fig. 2. Net rectangle for finite-difference approximations.

$$\delta u_j - \delta u_{j-1} - \frac{h_{j-1}}{2}\left(\delta f_j + \delta f_{j-1}\right) = (r_3)_{j-1} \tag{9a}$$

$$\frac{1}{h_{j-1}}(\delta v_j - \delta v_{j-1}) + (s_7)_j\,(\delta u_j + \delta u_{j-1}) = (r_1)_j \tag{9b}$$

$$(s_1)_j\delta f_j + (s_2)_j\delta f_{j-1} + (s_3)_j\delta v_j + (s_4)_j\delta v_{j-1} + (s_5)_j\delta u_j + (s_6)_j\delta u_{j-1} = (r_2)_j \tag{9c}$$

After linearization, the wall boundary conditions

$$u_o = 0, \qquad v_o = 0 \tag{10a}$$

and the edge boundary condition

$$u_J = u_e \tag{10b}$$

become

$$\delta u_o = 0, \qquad \delta v_o = 0, \qquad \delta u_J = 0 \tag{11}$$

The resulting linear system consisting of those given in Eqs. (9) and by those in Eq. (11) can be solved by the block elimination method discussed by Cebeci and Bradshaw[10].

## Solution Procedure for $t > 0$

We have already pointed out that if $\partial u_e/\partial t \neq 0$ when $t = 0$, a double structure scheme should strictly be used to advance the solution from $t = 0$. However the choice of parameters in our study is such that $\partial u_e/\partial t$ is small and the difficulties that arise from using a standard method are of a sufficiently minor nature that no further refinement is necessary. For larger values of the relevant parameters it is easy to incorporate a smoothing function into $u_e$ and one can always use the general method[2].

Nevertheless there is still the difficulty about obtaining the velocity profile on the first x-station at any new time-line. It can be resolved with the use of the characteristic box method developed by Cebeci and Stewartson[14]. Defining the streamline by

$$\frac{dt}{1} = \frac{dx}{u} \tag{12}$$

and using the definition of $f'$, and with $s$ denoting the local streamline, we write Eq. (4) as

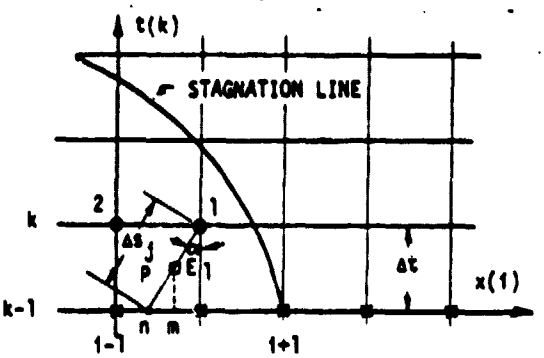


Fig. 3. Notation and finite-difference molecule for the Characteristic Box 2.

$$(bf') - fv + \sqrt{1 + u_e^2}\,\frac{\partial u_e}{\partial s} = \sqrt{1 + u^2}\,\frac{\partial u}{\partial s} \tag{13}$$

To obtain the solution of the unsteady boundary-layer equations given by Eqs. (7a,b) and (13) at the first x-station on either side of the stagnation line, let us consider the grid of Fig. 1 and direct our attention to the point denoted by 1 (see Fig. 3).

To write the difference approximations of Eq. (13) we define

$$\Delta s_j = \Delta t/\cos\alpha_j \tag{14}$$

where, with $u_j$ denoting an average velocity, we compute $\alpha_j$ from

$$\alpha_j = \tan^{-1} u_j \tag{15}$$

assuming that at first $v$ at point $P$ is known and is equal to its value at $v^{i-1/2,k-1}$. This assumption decouples the continuity equation, Eq. (7') from Eqs. (7a) and (13) and reduces the problem to a "two-dimensional" one with $f$ and $u$ being the only unknowns. The finite-difference approximations of Eq. (7a) are written in the usual way and the finite-difference approximations to Eq. (13) are written by centering it at point $P$. This procedure leads to

$$h_{j-1}^{-1}(f_j^{i,k} - f_{j-1}^{i,k}) - u_{j-1/2}^{i,k} = 0 \tag{16a}$$

$$\frac{(bv)_j^{i,k} - (bv)_{j-1}^{i,k}}{2h_{j-1}} + \frac{(bv)_j^{n,k-1} - (bv)_{j-1}^{n,k-1}}{2h_{j-1}} - \frac{1}{2}\left[f_{j-1/2}^{i,k} + f_{j-1/2}^{n,k-1}\right]\left[v_{j-1/2}^{P}\right]$$
$$+ \frac{1}{2}\left[\left(\sqrt{1+u_e^2}\right)^{i,k} + \left(\sqrt{1+u_e^2}\right)^{n,k-1}\right]\left(\frac{u_e^{i,k} - u_e^{n,k-1}}{\Delta s_j}\right)$$
$$= \frac{1}{2}\left[\left(\sqrt{1+u^2}\right)_{j-1/2}^{i,k} + \left(\sqrt{1+u^2}\right)_{j-1/2}^{n,k-1}\right]\frac{u_{j-1/2}^{i,k} - u_{j-1/2}^{n,k-1}}{\Delta s_j} \tag{16b}$$

The profiles $b_j$, $f_j$ and $u_j$ as well as $u_e$ at $(n,k-1)$ are obtained by interpolating the profiles at $(i,k-1)$ and $(i-1,k-1)$. To find the angle $\alpha_j$, we define $u_j$ in Eq. (15) by

$$u_j = \frac{1}{2}\left(u_j^{i,k} + u_j^{n,k-1}\right) \tag{17}$$

Since the system given by Eqs. (16) is linear, there is no need for linearization and we solve it subject to the two boundary conditions, namely,

$$u_o = 0, \qquad u_J = u_e \tag{18}$$

by using the block-elimination method in which case the matrices are 2 x 2. We shall refer to this scheme as Characteristic Box 2.

Once a solution of Eqs. (7a) and (13) has been obtained, we compute $v$ from Eq. (7b) which, in finite-difference form, for the center of the net rectangle, point E, can be written as (see Fig. 3)

$$\frac{V_j - V_{j-1}}{h_{j-1}} = -\frac{u_j^{i,k-1/2} - u_j}{x_i - x_m} \tag{19}$$

Here $V_j$ denotes the value of $v_j$ at E and $u_j$ is given by Eq. (17). Since the right-hand side of Eq. (19) is known, we can solve this equation for $V_j$ and with $V_o = 0$, find $V_j$ for $1 \leq j \leq J$. We then substitute this new value of $V_j$ into Eq. (16) for $v^p$ and solve the system again to compute new values of $V_j$. This procedure is repeated until convergence.

For convenience we use the same procedure to compute point 2 to the left of point 1. Once two points on a given t-line are computed by this procedure, we then use the values of $V_j$ at $E_2$ and $E_1$, compute a new value $v^p$ and repeat the solution procedure for Eqs. (7a) and (13), and later Eq. (19). After that the stations to the left of point 2 and the stations to the right of point 1 are computed by using the Regular Box scheme if there is no flow reversal across the layer and by the Characteristic Box scheme if there is flow reversal. The "new" Characteristic Box scheme is now slightly different than the Characteristic Box 2 so we shall refer to it as Characteristic Box 3.

To describe the Characteristic Box 3 scheme which solves Eqs. (7a,b) and (13) without decoupling the continuity equation from Eqs. (7a) and (13), we consider the sketch shown in Figure 4.

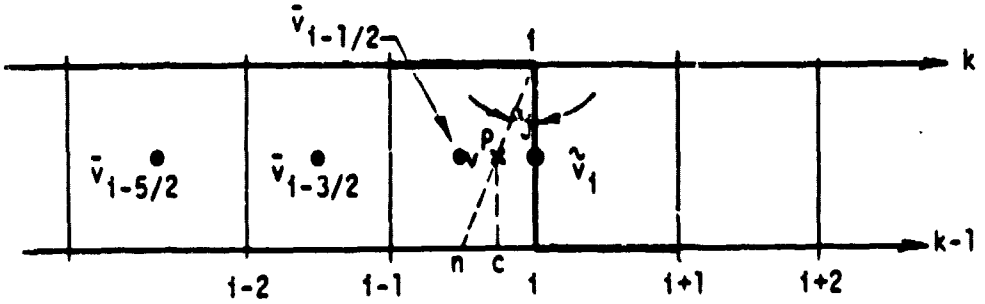


Fig. 4. Notation for Characteristic Box 3.

Using the Zig-Zag Box scheme discussed in detail in Ref. 5, we write Eq. (7b) in the following finite-difference form

$$h_{j-1}^{-1}\,(\tilde{v}_j^i - \tilde{v}_{j-1}^i) + \tilde{\theta} u_{j-1/2}^{i,k} = -\beta_1 + \tilde{\theta} u_{j-1/2}^{i-1,k} \tag{20}$$

where

$$\tilde{\theta} = \frac{(x_{i+1} - x_i)}{(x_{i+1} - x_{i-1})}\,\frac{1}{(x_i - x_{i-1})}\,,$$

$$\beta_1 = \frac{x_i - x_{i-1}}{x_{i+1} - x_{i-1}}\,\frac{1}{(x_i - x_{i+1})}\quad (u_{j-1/2}^{i,k-1} - u_{j-1/2}^{i+1,k-1}) \tag{21}$$

Since

$$\bar{v}_{i-1/2} = \bar{v}_{i-3/2} + \frac{(x_{i-1/2} - x_{i-3/2})}{(x_{i-3/2} - x_{i-5/2})}\,(\bar{v}_{i-3/2} - \bar{v}_{i-5/2}),$$

The relation between $\bar{v}_{i-1/2}$ and $\tilde{v}_i$ can be written as

$$\tilde{v}_i = (1 + \beta_2)\bar{v}_{i-1/2} + \beta_3 \tag{22}$$

where $\beta_2$ and $\beta_3$ are given by

$$\beta_2 = -\frac{(x_i - x_{i-1/2})}{(x_{i-3/2} - x_{i-1/2})}\,, \qquad \beta_3 = -\beta_2\bar{v}_{i-3/2} \tag{23}$$

Introducing Eq. (22) into Eq. (20) and rearranging, we get

$$h_{j-1}^{-1}\,(1 + \beta_2)(\bar{v}_j - \bar{v}_{j-1}) + \tilde{\theta} u_{j-1/2} = \beta_4 \tag{24}$$

where

$$\beta_4 = -\beta_1 + \tilde{\theta} u_{j-1/2}^{i-1,k} + h_{j-1}^{-1}\,(\beta_3^{j-i} - \beta_3^{i}) \tag{25}$$

As in Characteristic Box 2, we center Eq. (13) at the midpoint of (i,k) and (i,n) to get the finite-difference equations given by Eq. (16b) with $v^P$ being obtained by linear interpolation of $\tilde{v}_{i-1/2}$ and $\tilde{v}_i$, which is

$$v^P = \tilde{v}_i + (x_c - x_i)\,\frac{v_{i-1/2} - \tilde{v}_i}{x_n - x_i} \tag{26}$$

Equations (16a), (24) and (16b) are then linearized by Newton's method, and again are solved by the block elimination method.

When there is no flow reversal across the layer, we use the Regular Box scheme described in detail in Ref. 5.

## Results and Discussion

To date calculations have been carried out in only one test-case, namely when $\xi_0 = 0.10$, $A = 1$, $\omega = \pi/4$, and for a limited range of $x$ ( $|x| < 0.3$). With the use of the various procedures described in this paper the calculations were quite straightforward and the formal validity and efficacy of the numerical schemes were established. The results are summarized in Figs. 5-7. In Fig. 5 we display the variation of wall-shear with time at different x-stations and in Fig. 6 the variation with $x$ at different times. These graphs are entirely in line with expectations and we note that the flow reversal at the wall is quite smooth. A similar remark applies to the velocity profiles on either side of the stagnation line displayed in Fig. 7.

The next phase in our studies is to extend the computations to larger values of $A, \xi_0$ and smaller values of $\omega$ so as to more closely approach the conditions of dynamic stall. It is of interest to comment on the fluid mechanical problems that may then arise. First, if $\xi_0$ is increased beyond 1.155, the steady-state solution at $t = 0$ separates on the upper side of the airfoil and the calculation terminates. This is not a serious drawback unless the unsteady boundary develops a singularity because the smoothing function mentioned earlier may be adapted to ensure that $\xi_0$ is initially less than 1.155 and rises to a value greater than that after a finite time. The unsteady boundary layer then includes regions of reversed flow which may well become extensive if $A$ is also

allowed to increase to mimic more closely the conditions of dynamic stall. Even if the boundary layer remains smooth, the displacement thickness may then become much thicker and have a significant modifying effect on the external flow. It would be useful then to consider an interactive problem in which the external stream depends in part on the displacement thickness thus generalizing the studies reported for steady flow[7]. Consideration then has to be given to the variation of circulation with time which may lead to a more complicated expression for the dependence of $u_e$ on the displacement thickness than was used in Ref. 7 but the computation should not be any more complicated as a result. Finally, in order to mimic the dynamic stall problem most effectively[1,11], $\omega$ should be reduced to very small values (as typical of dynamic stall problem). So long as $\omega > 0$, the difficulties reported in Ref. 3 at separation in uninteracted flows and in post-separation flows otherwise, should not be present. On the other hand, van Dommelen and Shen[12] have provided quite strong evidence that a singularity can occur in an unsteady boundary layer for which the external velocity is steady. This phenomenon is still somewhat controversial[13] but there seems no doubt that the boundary layer will exhibit dramatic properties for small enough values of $\omega$ and it is possible that these may give further insight into dynamic stall.

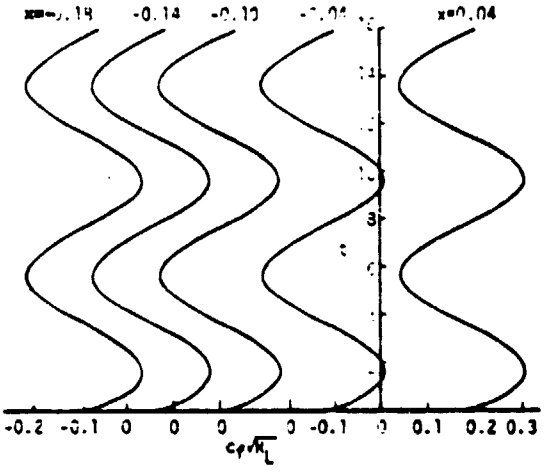


Fig. 5. Variation of wall shear parameters with time at different x-stations.

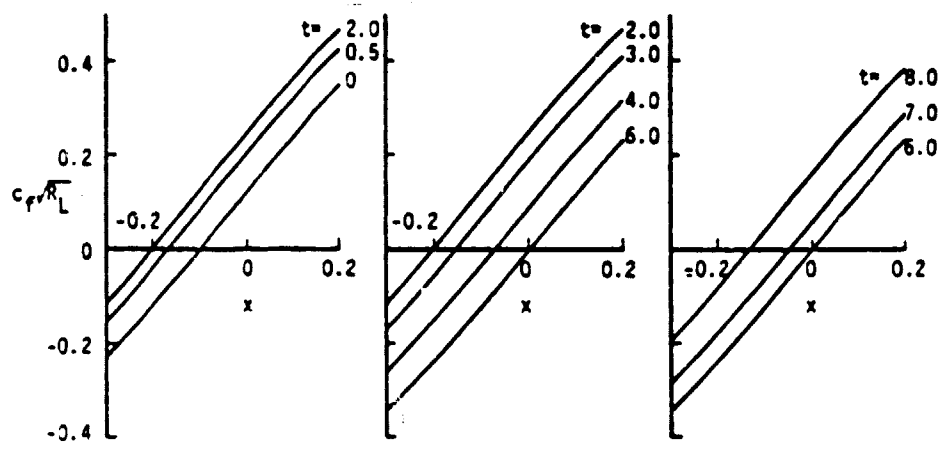


Fig. 6. Variation of skin-friction coefficient with $x$ at different t-intervals. Note $t = 8$ corresponds to one cycle.

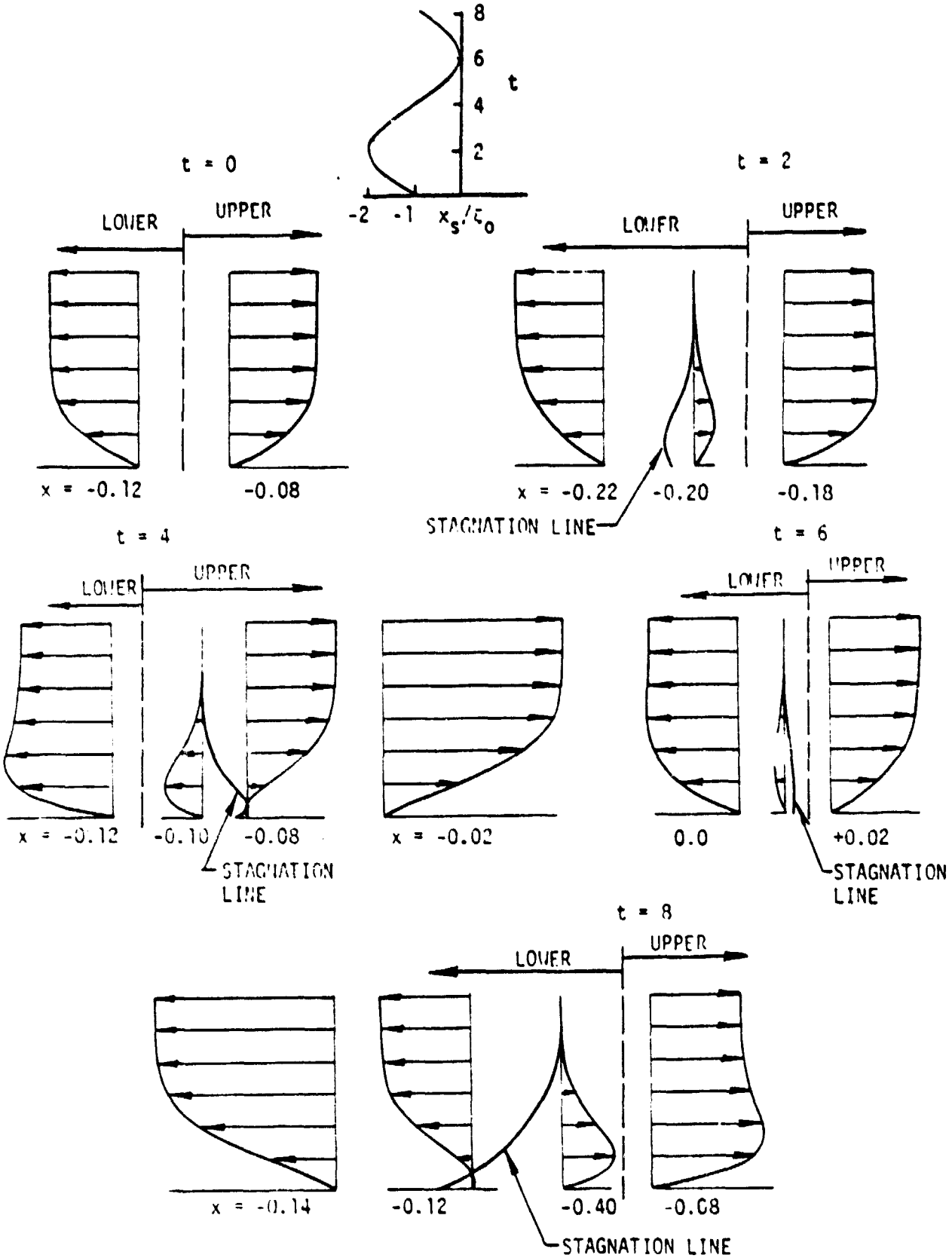


Fig. 7. Velocity profiles in the immediate neighborhood of the stagnation lines at different times. $u_e = 0$ on the dashed line at the specified time and serves to "define" upper or lower surfaces.

## References


1. Carr, L.W.; McAlister; K.W., and McCroskey, W.J.: Analysis of the development of dynamic stall based on oscillating airfoil experiments. NASA TN D-8382 (1977).

2. Cebeci, T.; Thiele, F.; Williams, P.G. and Stewartson, K.: On the calculation of symmetric wakes. I. Two-dimensional flows. Num. Heat Trans. 2, (1979) 35-60.

3. Cebeci, T.: The laminar boundary layer on a circular cylinder started impulsively from rest. J. of Comp. Phys., 3, No. 2, (1979).

4. Cebeci, T. and Stewartson, K.: Unpublished work (1978).

5. Cebeci, T. and Carr, L.W.: Computation of unsteady turbulent boundary layers with flow reversal and evaluation of two separate turbulence models. NASA TM 81259 (1981).

6. Cebeci, T.; Khattab, A.A. and Stewartson, K.: Three-dimensional laminar boundary layers and the ok of accessibility. To appear in J. Fluid Mech. (1981).

7. Cebeci, T.; Stewartson, K. and Williams, P.G.: Separation and reattachment near the leading edge of a thin airfoil at incidence. AGARD Symp. on Computation of Viscous-Inviscid Interacting Flows, Colorado Springs, Colo. (1980).

8. Cebeci, T. and Smith, A.M.O.: Analysis of Turbulent Boundary Layers. Academic Press, N.Y. (1974).

9. Bradshaw, P.; Cebeci, T. and Whitelaw, J.H.: Engineering Calculation Methods for Turbulent Flow. Academic Press, London (1981).

10. Cebeci, T. and Bradshaw, P.: Momentum Transfer in Boundary Layers. Hemisphere/McGraw-Hill, Washington, D.C. (1977).

11. McCroskey, W.J. and Pucci, S.L.: Viscous-inviscid interaction on oscillating airfoils. AIAA Paper No 81-0051, Jan. 1981.

12. VanDommelen, L.L. and Shen, S.F.: The genesis of separation. Proc. of Numerical and Physical Aspects of Aerodynamic Flows, California State University, Long Beach, January 19-21, 1981.

13. Cebeci, T.: Unsteady separation. Proc. of Numerical and Physical Aspects of Aerodynamic Flows, California State University, Long Beach, January 19-21, 1981.



Acknowledgment. This work was supported by NASA Ames under contract NAS2-10799. The authors would like to thank Professor Keith Stewartson for many helpful discussions on this problem and to Janet Chiu for her help in programming.